Rotational and Constitutional Dynamics of Caged Supramolecules

Dirk Kühne[1], Florian Klappenberger[1], Wolfgang Krenner[1], Svetlana Klyatskaya[2], Mario Ruben[2,3] and Johannes V. Barth[1]

[1] Physik Department E20, TU München, James-Franck Str., D-85748 Garching, Germany; [2] Institut für Nanotechnologie, Karlsruhe Institute of Technology, D-76021 Karlsruhe, Germany; [3] IPCMS-CNRS UMR 7504, Université de Strasbourg, 23 Rue du Loess, 67034 Strasbourg, France

The confinement of guest species in nanoscale environments leads to new dynamic phenomena. Notably the organisation and rotational motions of individual molecules were controlled by carefully designed, fully supramolecular host architectures. Here we use an open 2D coordination network on a smooth metal surface to steer the self-assembly of discrete trimeric guest units, identified as noncovalently bound dynamers. Each caged chiral supramolecule performs concerted, chirality-preserving rotary motions within the template honeycomb pore, which are visualized and quantitatively analyzed using temperature-controlled scanning tunneling microscopy. With higher thermal energies furthermore a constitutional system dynamics appears, that is revealed by monitoring repetitive switching events of the confined supramolecules' chirality signature, reflecting decay and reassembly of caged units.

Keywords: Self-assembly, supramolecular dynamics, nanochemistry, surface architecture.

The dynamics of molecular species can be controlled by carefully designed, fully supramolecular host architectures, provided either as discrete capsules or extended nanoporous networks. It was recognized in particular that unique rotary motion phenomena of single molecular species can be encoded by such conditions (1-5). Moreover, with the restriction to surface-confined systems, it became possible to investigate molecular rotation and non-covalent assembly processes of individual molecules adsorbed at surfaces by atomic-scale scanning tunneling microscopy (STM) (6-12). However, the direct observation of dynamic supramolecular entities in controlled environments remained elusive, although this represents a key issue of supramolecular science and constitutional dynamic chemistry (13-16). Herein we report novel dynamic phenomena at the supramolecular level, resulting from the nanoscale confinement of a multicomponent aggregate in an open 2D coordination network on a smooth metal surface. The presented nanopores steer the assembly and cage the realized discrete 2D-chiral trimeric dynamers, whose behaviour is directly monitored by temperature-controlled STM. We visualized and analyzed quantitatively their rotary motions, whereby the collective nature of the system dynamics is demonstrated by following chirality-preserving individual reorientation events, which findings reveal new opportunities for the field of surface-mounted rotors, limited to single molecular units so far (17-19). Furthermore we infer constitutional dynamics from the switching of the chirality signature for increased thermal energies, reflecting the repetitive decay and reassembly of the caged supramolecules. With our findings a demonstrator for the intricate collective dynamics of caged supramolecular dynamers is provided.

Results and Discussion

For our investigations we rely on the principles of surface-confined supramolecular chemistry, a versatile strategy for the fabrication of low-dimensional molecular architectures (20, 21). This methodology was notably employed to design regular nanoporous networks presenting well-defined and tunable cavities (22-25). Specifically, we employed the Co-directed assembly of linear ditopic *para*-hexaphenyl-dicarbonitrile (NC-Ph_6-CN) linkers to generate a highly regular array of well-defined host spaces on a smooth single crystal silver surface in (111) orientation under vacuum conditions (26). STM data of an exemplary network are depicted in

Fig. 1a, revealing the high regularity of the template providing hexagonal pores with an enclosed van der Waals area of 24 nm^2. The ideal stoichiometry for this room-temperature assembled network is given by a ratio of 3:2 of rod-like linkers and cobalt centers, respectively. However, upon increasing the surface concentration of the linkers at reduced temperatures (~ 145 K), they are captured in the network cavities because the energy barrier to migrate across the network rims is high enough to limit intercavity mass transport, which eventually sets in at T ~ 165 K.

The confined molecules are free to arrange within the pore in energetically favorable configurations. The outcome of such an experiment following the network exposure to an additional 0.1 monolayer linker concentration and subsequent cool-down to a temperature of eight kelvins is shown by the STM image reproduced in Fig. 1b (for an overview image, see Fig. S1 in the supplementary information (SI) appendix). Firstly, we note that the confined monomers are always attached to the network rim in a specific geometry, reflecting a surface templating effect and weak attractions between phenyl hydrogen and CN endgroups. This arrangement is consistent with the structural motifs observed in pure organic lattices of linear dicarbonitrile linker molecules on the same surface (27, 28). Secondly, we identify a frequent trimeric arrangement reflecting the self-assembly of three caged linkers. Here a new threefold nodal bonding motif is encountered at the center of the trimeric unit, which must be understood as a consequence of the spatial confinement, because in organic layers exclusively fourfold nodal motifs exist (27, 28). Nevertheless, there is again a preferred registry of the supramolecular trimer with respect to the surface atomic lattice, i.e., the molecular backbones are oriented along close-packed <1-10> directions and the terminating nitrogen atoms reside at threefold hollow sites (ref. (28); cf. Fig. 1c and the model S2a in the SI appendix). In addition cavities exist that are either undecorated or host merely one molecule or arrangements of two or four guest molecules. Furthermore, Fig. 1b evidences, that there are two mirror-symmetric configurations of the supramolecular trimer reflecting an organisational chirality (27, 28). These enantiomorphous species are designated λ- and δ-rotator, respectively. Because these supramolecules will be shown to undergo thermally activated collective motions and continuous changes in their constitution they are recognized as *dynamers* (16).

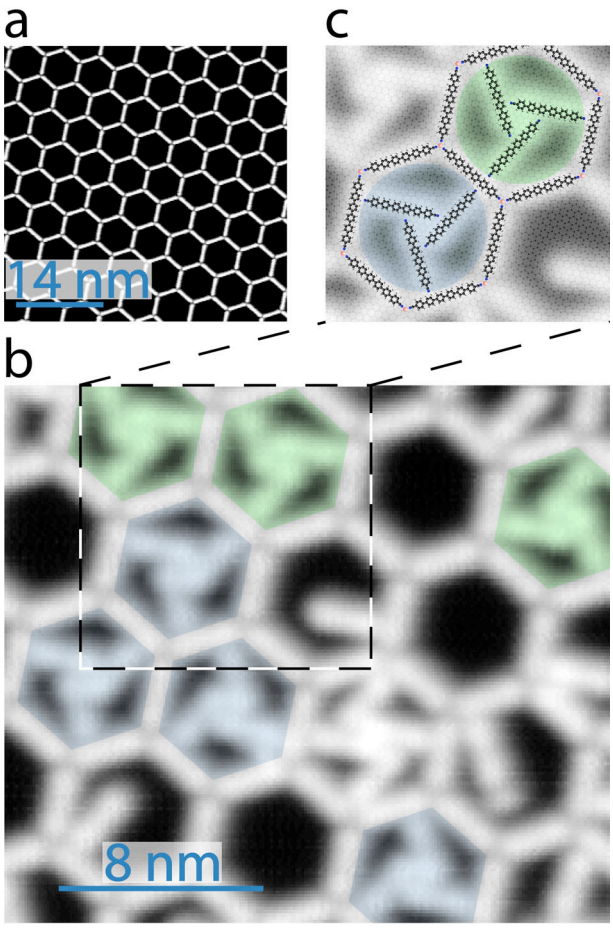

Fig. 1: Supramolecular chiral trimers in a nanoporous host lattice. **a** The template is provided by a regular 2D coordination network on a Ag(111) surface. The van der Waals area of the provided cavities is 24 nm^2 (V_B = 0.5 V, I_T = 0.1 nA, T_{Sample} = 8 K). **b** Self-assembled supramolecular trimers in two chiral configurations marked with blue and green hexagons named λ- and δ-rotator, respectively (V_B = 2.0 V, I_T = 0.1 nA, T_{Sample} = 29 K). **c** Structure model of the caged trimers that are stabilised by weak bonds between carbonitrile endgroups and phenyl moieties (H, C, N and Co atoms in white, black, blue and red, respectively).

Altogether the situation reflects a two-level assembly of a 2D host network with caged supramolecular chiral guests, the shape of which is determined by the balance of intermolecular, molecule-surface and host-guest interactions. Now, the metal-organic honeycomb nanomesh is thermally robust because of the underlying metal-ligand interactions that determine its structure (23, 24). By contrast, the lateral bonding of the guest system, both regarding its internal structure and its attachment to the host cavity implies weaker, non-covalent interactions. In order to probe its response to thermal excitations, repeated STM measurements with increasing temperatures have been performed. Starting at T ~ 25 K, we continuously imaged approximately 175 cavities during several days. At T ~ 60 K, the first indications of thermal motions of the guest unit appeared. Importantly, they concern the entire supramolecular unit. Typical rotation events are visualized by the data series in Figs.

2a-c concentrating on a single caged δ-rotator. It is obvious that an orientation switching event occurred in the time interval between the recording of the images (a) and (b). This corresponds to a transition between energetically equivalent but geometrically different configurations with an identical chirality signature. The pertaining states are designated δ_1, δ_2 and λ_1, λ_2, respectively.

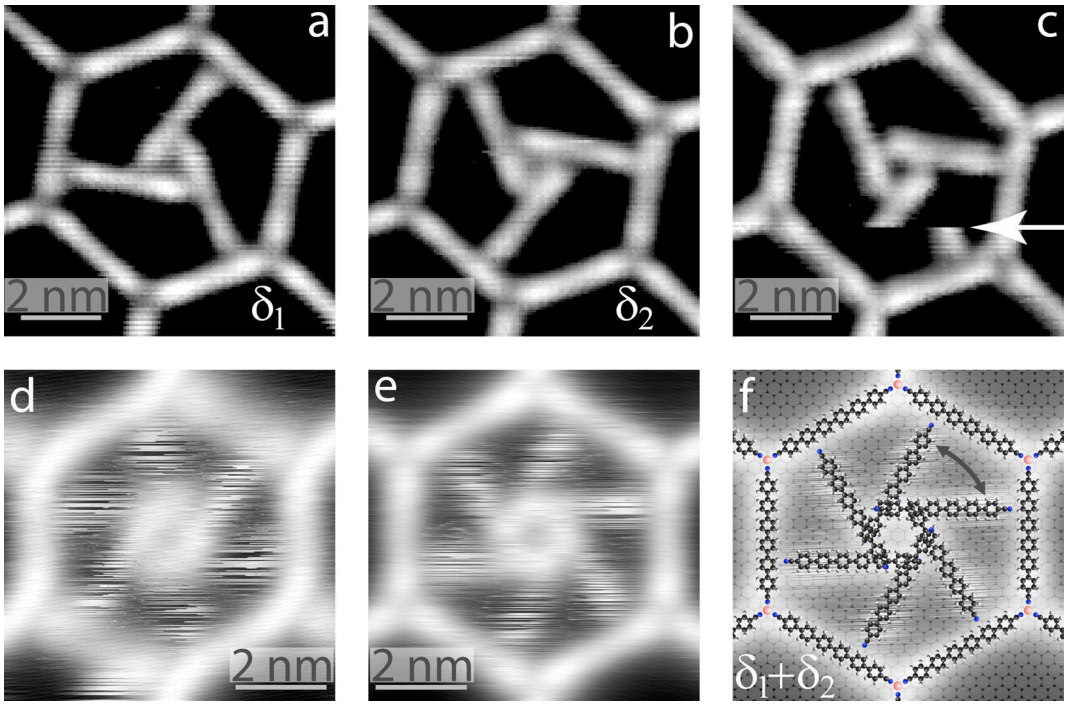

Fig. 2: Rotational motion of the caged supramolecular dynamer. **a,b** 60° orientational switching between a stable δ_1 and δ_2 configuration with conservation of the chirality signature; images recorded with a time lap of 204 s (V_B = 1.0 V, I_T = 0.05 nA, T_{Sample} = 64.4 K). **c** Orientation switching event while recording the topography at the position indicated with an arrow; the molecular units are exclusively imaged with positions reflecting preferred configurations (V_B = -1.0 V, I_T = 0.05 nA, T_{Sample} = 64.8 K). **d,e** Rapid fluctuation of rotator states with event rates largely exceeding imaging frequency. The envelope of the intracavity molecular features with different chirality corresponds to a superposition of the two respective stable configurations ((d): λ-rotator, V_B = -1.0 V, I_T = 0.1 nA, T_{Sample} = 78.3 K, (e): δ-rotator, V_B = 0.2 V, I_T = 0.22 nA, T_{Sample} = 81 K). **f** Model for the collective rotation superimposed on the data in (e).

A further chirality-conserving event occurred during the scanning of the rotator within the measurement process. It is marked by an arrow in Fig. 2c and reveals that the time for the repositioning of the unit is much smaller than the interval for the recording of a linescan (164 ms). Furthermore, looking at well more than thousand rotator images we found no indications of intermediate configurations of the rotator, suggesting that the orientational switching corresponds to a collective rotation of the entire supramolecular trimeric unit. This interpretation, in contrast to the principally existing possibility of sequential motions of individual molecular units in rapid succession, is

supported by the fact, that the elements of the supramolecular unit cannot be individually displaced between positions of different rotary configurations because of steric hindrance. The pertaining model shown in Fig. 2f (for more detailed views see Figs. S3b-d of the SI) reveals that the reason is the proximity of the carbonitrile groups and phenyl rings, i.e., the supramolecular bonding motif. A sequential motion would entail distances between molecular moieties falling locally below the van der Waals spheres of the constituents. The idea of a concerted rotational motion is corroborated by observations at higher temperatures, where it is impossible to image a static rotator because of the increased rotation rates. Under these conditions frizzled features are resolved in the cavities indicating rapid thermal motions (cf. Figs. 2d,e). In agreement with earlier STM observations of single rotating molecules (10, 29-31), this imaging is ascribed to a unit rapidly rotating in arbitrary directions while residing on the average at the preferred surface orientations. With the present system, the envelope of the intracavity molecular features accordingly corresponds exactly to the superposition of the two distinguishable rotator orientations (cf. Figs. 2a-f). Importantly, this holds independently for both mirror-symmetric species (cf. Figs. 2d,e), i.e., there is again chirality conservation in agreement with the notion of a supramolecular unit performing concerted motions. Thus the hexagonal cavity dictates the shape of the self-assembly geometry and acts simultaneously as a supramolecular stator for the confined rotary motion of the dynamer exhibiting in this case only rotational but no constitutional dynamics.

On the basis of the systematic temperature-controlled STM data sets we performed a statistical analysis of the rotational switching event rates (details on the procedures are given in the methods section; in short, they follow methodologies established for molecular surface diffusion, see ref. (32)). The results are plotted in the Arrhenius representation reproduced in Fig. 3. They show the characteristics of a thermally activated process described by the well-known formula $\Gamma_{rot} = A \exp[-E_{rot}/(kT)]$, where Γ_{rot} represents the rotation rate, A the prefactor, and E_{rot} the rotational energy barrier. A corresponding fit to the data yields : $E_{rot} = 187 \pm 8$ meV and $A = 1.3 (\pm 0.8) \times 10^{12}$ s^{-1}.

Thus the strictly surface-confined self-assembly approach, using instructed molecular bricks, leads to the parallel construction of stator-rotator assemblies, which show inherently self-adaptation to the specific near-surface working conditions. The

straightforward use of the self-assembly techniques in the architectural design cannot only provide direct access to functional surface structures, it also reflects the highly supramolecular design principles ubiquitary found in biological motors (e.g. rotary ATPase, linear kinesine and myosine motors).

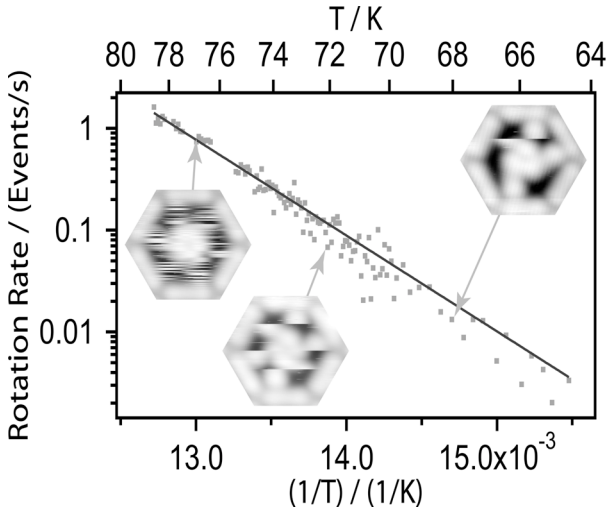

Fig. 3 Arrhenius plot of dynamer rotation event rates. The data obey the expression $\Gamma_{rot} = A \exp[-E_{rot}/(kT)]$, the line fit yields: A = 1.3 (± 0.8) × 10^{12} s^{-1}, E_{rot} = 187 ± 8 meV. Insets show exemplary STM images with a caged rotator in a single cavity at different temperatures (recorded with V_B = 2.0 V, I_T = 0.1 nA).

With substrate temperatures exceeding ~70 K, intracavity chirality interconversion sets in as a rare event, as exemplified by the data reproduced in Fig. 4. Similar to the rotation events these transitions are much faster than the instrumental scanning speed. Thus they cannot be visualized directly, but can be tracked by the change of the chirality of a rotator. In the presented case, a λ-rotator (Fig. 4a, trimer on the right) transforms into a δ-rotator (Fig. 4b, trimer on the right). As a consequence, at even higher temperatures the rotator STM appearance undergoes a qualitative change. Instead of frizzled features discussed above a rather smooth, albeit slightly blurred envelope, of the intracavity molecular features occurs (Fig. 5a, recorded for T = 145 K).

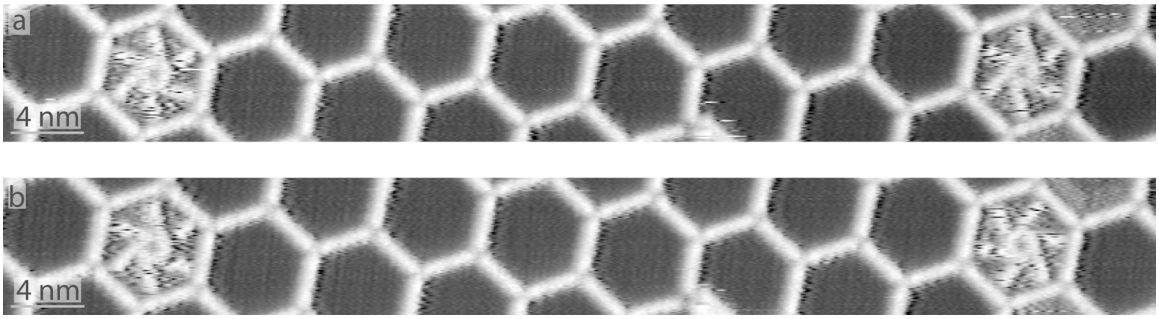

Fig. 4: Simultaneous observation of two dynamic caged rotators with equal (**a**) and opposite (**b**) handedness; images recorded with a time lap of 340 s (V_B = -2.07 V, I_T = 0.05 nA, T_{Sample} = 90.5 K). Between the two images of the same surface area an intracavity chirality interconversion occurred as a rare event.

The novel appearance is understood as a consequence of averaging over many thermal motion processes that occur in the cavity during the recording of each individual scan line. At these conditions, the level of thermal excitation does not allow the caged molecules to migrate across the cavity rims, whence they remain spatially confined. However, the unique chirality signature of the rotators observed at lower temperatures has disappeared and a mirror-symmetric superposition figure prevails. The high number of cavities featuring identical envelopes is consistent with the number occupied by the trimeric dynamers at lower temperatures. This figure can be constructed from the superposition of all four possible rotator configurations (λ_1, λ_2, δ_1, and δ_2) combining both dynamic imaging features for rotators with different chirality (cf. Fig. 5b). The fact that the overall dynamic envelope of the confined linkers can be constructed this way confirms that this interconversion of rotor chirality, necessarily requiring a transient decay and reassembly of the rotator unit, occurs regularly at the employed temperatures. This is a clear indication for constitutional dynamics (16), i.e., there is a repetitive dissociation and reconstitution of the caged trimeric unit. In turn, the conservation of chirality throughout a large number of rotation events indicates that the collective rotary dynamics, i.e., *not* involving decay and re-assembly, persists over periods of time between the constitutional changes. In the temperature window 90.7 ± 0.4 K we measured a rate of $\Gamma_{chir} \approx 1.8 \times 10^{-3}$ s^{-1} for intracavity chirality switches (cf. Fig. 4). The corresponding rotation rate is 56.5 s^{-1}. Assuming a Markov process, where every second decay of the trimeric unit actually leads to a chirality switch, this means a ratio of rotation to decay rates of approximately 1.6×10^4. Using the same prefactor for both rotation and

decay, the activation barrier for the latter is estimated to $E_{decay} = kT \times \ln[A/(2\Gamma_{chir})] \approx$ 260 meV.

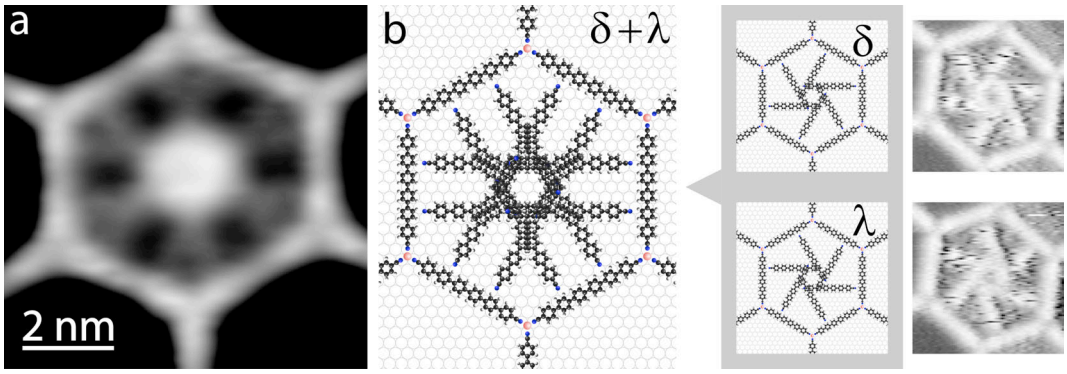

Fig. 5: Constitutional dynamics expressed in chirality switching of the caged trimeric unit. The blurred STM imaging is a result of intracavity decay and reassembly proceeding in parallel with rapid rotational motion of the caged dynamer. (**a**) The envelope of the intracavity molecular features reflects a superposition of the two enantiomers (δ and λ) of the chiral rotator (V_B = 0.5 V, I_T = 0.1 nA, T_{Sample} = 145 K), as demonstrated by the model in (**b**).

In the course of our systematic studies, there were no hints on a correlated occupation or dynamics of guest species in neighboring cavities, although this point can unfortunately not be conclusively addressed with the data sets at hand. Note that in several previous studies addressing single-molecule rotational motions in 2D superlattices correlations could also not be found for species confined in separate network cavities (9, 10). For an interesting example of a nanoporous template with communicating cavities, see ref. (33); however with this system the flexibility of the constituting porphyrins plays an important role. A potential pathway that could mediate a correlated dynamics is given by the indirect electronic interactions due to surface state scattering on the network and confined objects, which has been exploited to steer the alignment of adatoms in supramolecular gratings on the same substrate in the past (34, 35). However, with these systems there was similarly no evidence for a correlated translational motion or lateral organization in adjacent 1D furrows (34, 35), presumably because there is little crosstalk between areas separated by supramolecular boundaries (34-36).

Finally, we briefly comment on the nature and dynamics of single, dimeric and tetrameric guest arrangements. The data reproduced in the SI (Fig. S4) shows a single trimeric dynamer with adjacent cavities comprising the other species. At the employed conditions (temperature in the 60 – 61 K range), the monomers are already highly mobile and the filled cavity shows a streaky interior indicative of rapid

motions. In contrast, the rates for the thermal motions of dimers and tetramers are comparable to that of the trimer, whence thermally induced rearrangements of the confined supramolecules can be monitored. However, a detailed data analysis reveals that these motions frequently comprise both rotary and translatory steps, i.e., there are frequent structural changes of the supramolecular units. Consequently their dynamics cannot be described by the straightforward terms used for the trimer concerted rotary motions and constitutional rearrangements.

Conclusion

In conclusion, we demonstrated the bottom-up construction of caged supramolecular dynamers. Using a tailored nanoporous network as a template, we developed a hierarchic organization to generate collective motion and assembly phenomena with noncovalently designed chiral units. The realized supramolecular dynamers exert complex, concerted rotations, which have been directly monitored at the single-molecule level. In order to gain improved control over 2D supramolecular stator-rotator systems, e.g., achieving directionality, or changing the energy supply from heat to photons or electrons, synthesis and incorporation of responsive rotator units is envisioned. Furthermore, the observed chirality switching events of the caged trimeric units reflect a constitutional dynamics of the system, i.e., there is direct evidence of a dynamic chemistry at the supramolecular level. Our findings demonstrate the remarkable potential of surface-confined self-assembled nanoporous architectures by exploiting massively parallel fabrication concepts (20-25), to control dynamic phenomena of supramolecular species, here mechanically, but prospectively also concomitant electronic or magnetic dynamic features, e.g. mechano-electronic coupling of molecular motion with dynamic electron confinement.

Methods

The synthesis of the rod-like NC-Ph_6-CN molecule as well as the Co-directed honeycomb network assembly have been described in a previous publication (cf. ref. (26)). All experiments were performed under ultra-high vacuum conditions using a home-built liquid-He-cooled low-temperature STM with cryoshields (37). The employed Ag(111) substrate was prepared by standard procedures (cycles of Ar^+ sputtering and annealing) to obtain extended flat terraces separated by monoatomic steps. The linkers were deposited from a quartz crucible in an organic molecular beam

epitaxy source at 572 K, with the substrate kept at 300 K. Submonolayer molecular films were subsequently exposed to a beam of Co atoms for coordination assembly, whereby the linker to metal ratio was adjusted to 3:2. The Co-coordinated assembly was cooled down and an additional 0.1 monolayer concentration of linker molecules were added at 144 K (coverages are given with respect to the saturated monolayer coverage of a purely organic layer as defined in ref. (28)). Following the preparation the sample was transferred *in situ* and STM data were acquired at T = 8-150 K. During the measurements the tunneling parameters were in the high-resistance regime of 20 GΩ to avoid tip-induced motions.

The rotation rates were determined by counting the number of rotations within a hexagonal cavity and dividing this number by the time it took to scan the cavity. For low temperatures rotation events rarely happened. In this case their number was divided by the accumulated time, which elapsed while scanning the hexagonal cavity in between the occurrence of rotation events.

Acknowledgements

Work supported by the European Science Foundation Collaborative Research Program FunSMARTs, Center for Functional Nanostructures Karlsruhe (DFG-CFN Project E3.5), IGSSE and IAS at TU München, ERC Advanced Grant MolArt (°247299).

References

1. Rebek Jr., J. (2009) Molecular behavior in small spaces *Acc. Chem. Res.* 42: 1660 - 1668.
2. Kitagawa, H., Kobori, Y., Yamanaka, M., Yoza, K., Kobayashi, K. (2009) Encapsulated-guest rotation in a self-assembled heterocapsule directed toward a supramolecular gyroscope *Proc. Nat. Acad. Sci.* 106: 10444-10448.
3. Rosi, N. L., Eckert, J., Eddaoudi, M., Vodak, D. T., Kim, J., O'Keeffe, M., Yaghi, O. M. (2003) Hydrogen storage in microporous metal-organic frameworks *Science* 300: 1127 - 1129.
4. Horike, S., Shimomura, S., Kitagawa, S. (2009) Soft porous crystals *Nature Chem.* 1: 695 - 704.
5. Akutagawa, T., Koshinaka, H., Sato, D., Takeda, S., Noro, S.-I., Takahashi, H., Kumai, R., Tokura, Y., Nakamura, T. (2009) Ferroelectricity and polarity control in solid-state flip-flop supramolecular rotators *Nature Mat.* 8: 342-347.
6. Gimzewski, J. K., Joachim, C., Schlittler, R. R., Langlais, V., Tang, H., Johannsen, I. (1998) Rotation of a single molecule within a supramolecular bearing *Science* 281: 531 - 533.

7. Lin, N., Dmitriev, A., Weckesser, J., Barth, J. V., Kern, K. (2002) Real-time single-molecule imaging of the formation and dynamics of coordination compounds *Angew. Chem. Int. Ed.* 41: 4779 - 4883.
8. Kühnle, A., Linderoth, T. R., Hammer, B., Besenbacher, F. (2002) Chiral recognition in dimerization of adsorbed cysteine observed by scanning tunneling microscopy *Nature* 415: 891-893.
9. Schull, G., Douillard, L., Fiorini-Debuisschert, C., Charra, F., Mathevet, F., Kreher, D., Attias, A.-J. (2006) Single-molecule dynamics in a self-assembled 2D molecular sieve *Nano Lett.* 6: 1360.
10. Wintjes, N., Bonifazi, D., Cheng, F., Kiebele, A., Stöhr, M., Jung, T., Spillmann, H., Diederich, F. (2007) A supramolecular multiposition rotary device *Angew. Chem. Int. Ed.* 46: 4089 - 4092.
11. Tomba, G., Lingenfelder, M., Costantini, G., Kern, K., Klappenberger, F., Barth, J. V., Colombi Ciacchi, L., De Vita, A. (2007) Structure and energetics of diphenylalanine self-assembling on Cu(110) *J. Phys. Chem A* 111: 12740 - 8.
12. Grill, L., Rieder, K.-H., Moresco, F., Rapenne, G., Stojkovic, S., Bouju, X., Joachim, C. (2007) Rolling a single molecular wheel at the atomic scale *Nature Nanotechn.* 2: 95 - 98.
13. Lehn, J. M. (2002) Toward complex matter: supramolecular chemistry and self-organization *Proc. Nat. Acad. Sci.* 99: 4763-4768.
14. Rowan, S. J., Cantrill, S. J., Cousins, G. R. L., Sanders, J. K. M., Stoddart, J. F. (2002) Dynamic Covalent Chemistry *Angew. Chem. Int. Ed.* 41: 898-952.
15. Garcia-Garibay, M. A. (2005) Crystalline molecular machines: Encoding supramolecular dynamics into molecular structure *Proc. Nat. Acad. Sci.* 102: 10771 - 10776.
16. Lehn, J. M. (2007) From supramolecular chemistry towards constitutional dynamic chemistry and adaptive chemistry *Chem. Soc. Rev.* 36: 151 - 160.
17. Kottas, G. S., Clarke, L. I., Horinek, D., Michl, J. (2005) Artificial molecular motors *Chem. Rev.* 105: 1281-1376.
18. Browne, W. R., Feringa, B. L. (2006) Making molecular machines work *Nature Nanotechn.* 1: 25 - 35.
19. Balzani, V., Credi, A., Venturi, M. (2008) Molecular Machines Working on Surfaces and at Interfaces *ChemPhysChem* 9: 202 - 20.
20. Barth, J. V. (2007) Molecular architectonic on metal surfaces *Annu. Rev. Phys. Chem.* 58: 375 - 407.
21. Lin, N., Stepanow, S., Ruben, M., Barth, J. V. (2009) Surface-confined supramolecular coordination chemistry *Top. Curr. Chem.* 287: 1-44.
22. Theobald, J. A., Oxtoby, N. S., Phillips, M. A., Champness, N. R., Beton, P. H. (2003) Controlling molecular deposition and layer structure with supramolecular surface assemblies *Nature* 424: 1029 - 1031.
23. Stepanow, S., Lingenfelder, M., Dmitriev, A., Spillmann, H., Delvigne, E., Lin, N., Deng, X., Cai, C., Barth, J. V., Kern, K. (2004) Steering molecular organization and host-guest interactions using tailor-made two-dimensional nanoporous coordination systems *Nature Mat.* 3: 229-233.
24. Schlickum, U., Decker, R., Klappenberger, F., Zoppellaro, G., Klyatskaya, S., Ruben, M., Silanes, I., Arnau, A., Kern, K., Brune, H., Barth, J. V. (2007) Metal-organic honeycomb nanomeshes with tunable cavity size *Nano Lett.* 7: 3813 - 3817.

25. Madueno, R., Räisänen, M. T., Silien, C., Buck, M. (2008) Functionalizing hydrogen-bonded surface networks with self-assembled monolayers *Nature* 454: 618.
26. Kühne, D., Klappenberger, F., Schlickum, U., Decker, R., Brune, H., Klyatskaya, S., Ruben, M., Barth, J. V. (2009) High-quality 2D metal-organic coordination network providing giant cavities within mesoscale domains *J. Am. Chem. Soc.* 131: 3881-3883.
27. Schlickum, U., Decker, R., Klappenberger, F., Zoppellaro, G., Klyatskaya, S., Auwärter, W., Neppl, S., Kern, K., Brune, H., Ruben, M., Barth, J. V. (2008) Chiral kagomé lattice from simple ditopic molecular bricks *J. Am. Chem. Soc.* 130: 11778 - 11782.
28. Kühne, D., Decker, R., Klappenberger, F., Schlickum, U., Brune, H., Zoppellaro, G., Klyatskaya, S., Ruben, M., Barth, J. V. (2009) Self-assembly of nanoporous chiral networks with varying symmetry from sexiphenyl-dicarbonitrile on Ag(111) *J. Phys. Chem. C* 113: 17851 - 17859.
29. Maksymovych, P., Sorescu, D. C., Dougherty, D. B., Yates Jr., J. T. (2005) Surface bonding and dynamical behavior of the CH_3SH molecule on Au(111) *J. Phys. Chem. B* 109: 22463 - 22468.
30. Gao, L., Liu, Q., Zhang, X. Y., Jiang, N., Zhang, H. G., Cheng, Z. H., Qiu, W. F., Du, S. X., Liu, Y. Q., Hofer, W. A., Gao, H.-J. (2008) Constructing an array of anchored single-molecule rotors on gold surfaces *Phys. Rev. Lett.* 101: 197209.
31. Baber, A. E., Tierney, H. L., Sykes, E. C. H. (2008) A quantitative single-molecule study of thioether molecular rotors *ACS Nano* 2: 2385 - 2391.
32. Barth, J. V. (2000) Transport of adsorbates at metal surfaces : From thermal migration to hot precursors *Surf. Sci. Rep.* 40: 75-149.
33. Spillmann, H., Kiebele, A., Jung, T. A., Bonifazi, D., Cheng, F., Diederich, F. (2006) A two-dimensional porphyrin-based porous network featuring communicating cavities for the templated complexation of fullerenes *Adv. Mater.* 18: 275-279.
34. Pennec, Y., Auwärter, W., Schiffrin, A., Weber-Bargioni, A., Riemann, A., Barth, J. V. (2007) Self-assembled molecular superlattices for tunable confinement of electrons on metal surfaces *Nature Nanotechn.* 2: 99 - 103.
35. Schiffrin, A., Reichert, J., Auwärter, W., Jahnz, G., Pennec, Y., Weber-Bargioni, A., Stepanyuk, V. S., L. Niebergall, Bruno, P., Barth, J. V. (2008) Self-aligning atomic strings in surface-supported biomolecular gratings *Phys. Rev. B* 78: 035424.
36. Klappenberger, F., Kühne, D., Krenner, W., Silanes, I., Arnau, A., Garcìa de Abajo, F. J., Klyatskaya, S., R., M., Barth, J. V. (2009) Dichotomous array of chiral quantum corrals by a self-assembled nanoporous kagomé network *Nano Lett.* 9: 3509 - 3514.
37. Clair, S., Pons, S., Seitsonen, A. P., Brune, H., Kern, K., Barth, J. V. (2004) STM study of terephthalic acid self-assembly on Au(111): Hydrogen-bonded sheets on an inhomogenous substrate *J. Phys. Chem. B* 108: 19392-19397.

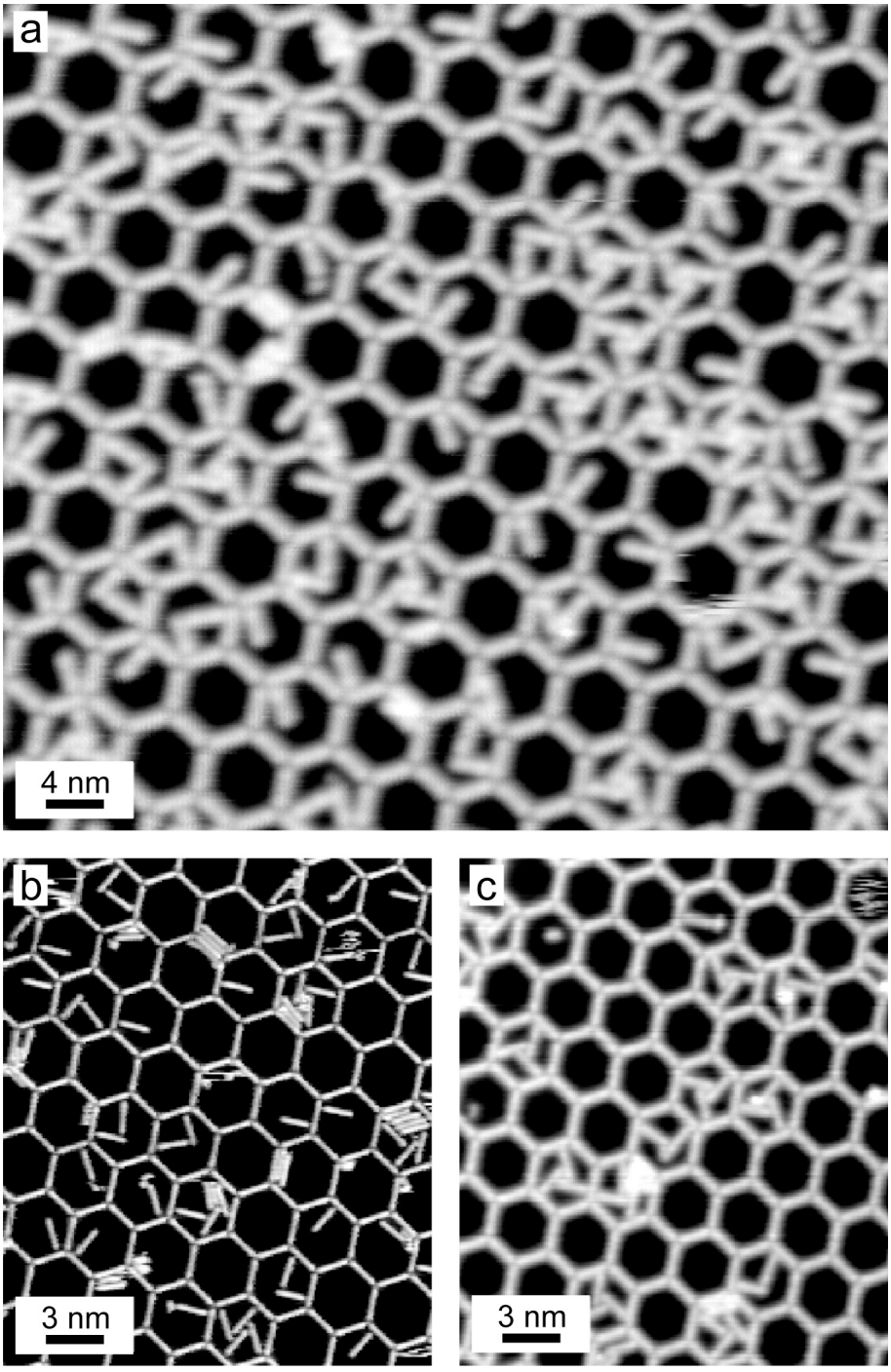

Fig. S1: (**a**) Overview image (62 nm × 58 nm) of the metal-organic host lattice after a concentration of 0.1 monolayers linker molecules has been added at 144 K. The additional molecules form monomers, dimers, trimers and tetramers, which all connect to the cavity rim. The available data does not indicate a statistically significant preference for clustering of rotators units in neighboring pores. In contrast to the trimers, whose components exhibit always the same alignment relative to each other, the dimers adopt different configurations, whereby the angle enclosed by the two molecules varies. (V_B = 2 V, I_T = 0.1 nA, T_{Sample} = 28.7 K). (**b**) A sample, where additional linker molecules were added at 130 K to the honeycomb template shows an appreciable concentration of single linker molecules and dimers in pores. (V_B = -0.58 V, I_T = 0.07 nA, T_{Sample} = 8 K) (**c**). The same sample after

annealing for 15 minutes at 165 K (V_B =1 V, I_T = 0.1 nA, T_{Sample} = 8 K). The fraction of linker guest molecules in trimeric rotator arrangements has increased from ~13% before annealing to ~50% after annealing, whereby only defect-free and undisturbed configurations were taken into account. This points to a threshold temperature for mass transport across the molecular barriers of the host lattice in the 150 - 160 K range. In addition, this evidences also the possibility of controlling the trimeric rotator fraction although this procedure has not been optimized within the present study.

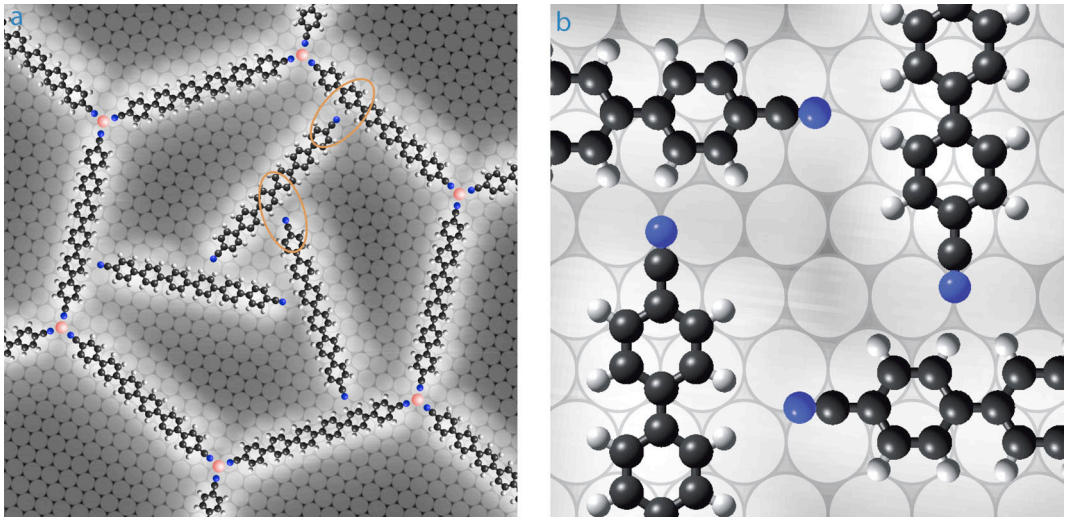

Fig. S2: (**a**) Bonding motifs and substrate registry of the caged rotator unit and (**b**) comparison with organization in a pure organic superlattice on the same surface (cf. D. Kühne *et al.*, *J. Phys. Chem. C* **113**, 17851 - 17859 (2009)). The same registry with the underlying atomic lattice, i. e., the carbonitrile group positioned on bridge or hollow sites and the long molecular axes oriented along <1-10> directions, is present in the rotator trimer and the fourfold node (the latter includes also molecules oriented along <11-2> directions). The lateral bonding of the rotator trimer (highlighted with orange ellipses) implies different hydrogen atoms of the molecule than that of the pure organic network.

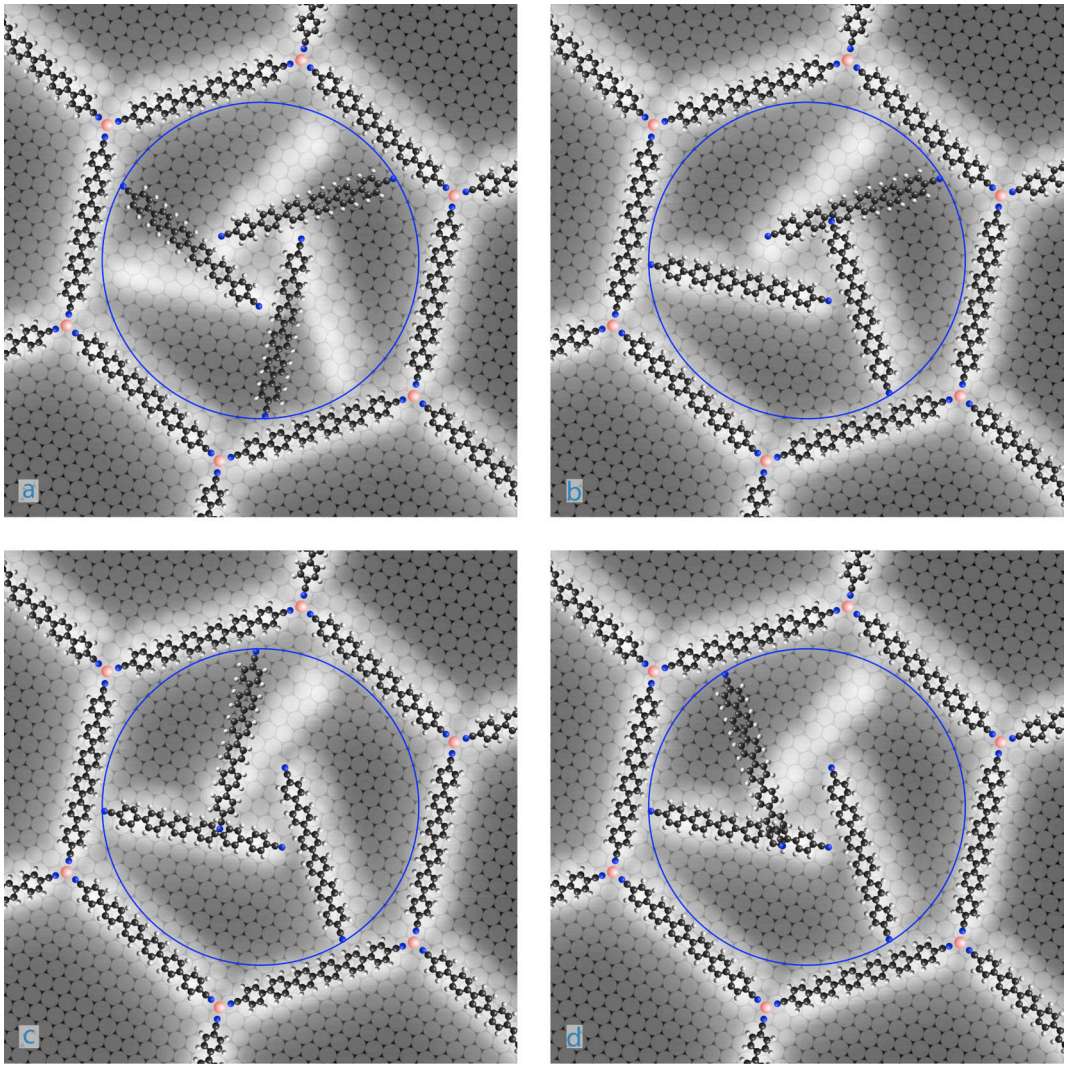

Fig. S3: (a) The caged rotator is not found to be rotated by 30° from its stable position, because the carbonitrile groups are no longer on a preferred bridge or hollow site. Rather, they would reside at substrate top positions as demonstrated by the model shown next to the observed stable configuration (light: STM appearance, V_B = 1.06 V, I_T = 0.1 nA, T_{Sample} ≈ 8 K).
(b-d) Steric hindrance prevents from a sequential movement of single units in the rotary motions of the supramolecular trimer. (b) The model shows a trimer whose threefold rotational symmetry is broken. Independently, one molecule has been rotated 30° degree clockwise around the center of rotation, which requires the rupture of the hydrogen bond with the molecule located counterclockwise. However, this positioning is not allowed physically because of the steric limitation set by the carbonitrile group and the phenyl moieties of the adjacent molecule located clockwise. (c) Analogous situation to the one depicted in the previous image, with one molecule rotated 30° counterclockwise. (d) Analogous situation with one molecule rotated 60° counterclockwise around the center of rotation, showing the impossibility of this configuration in a hypothetical sequential motion (stacking of molecules excluded).

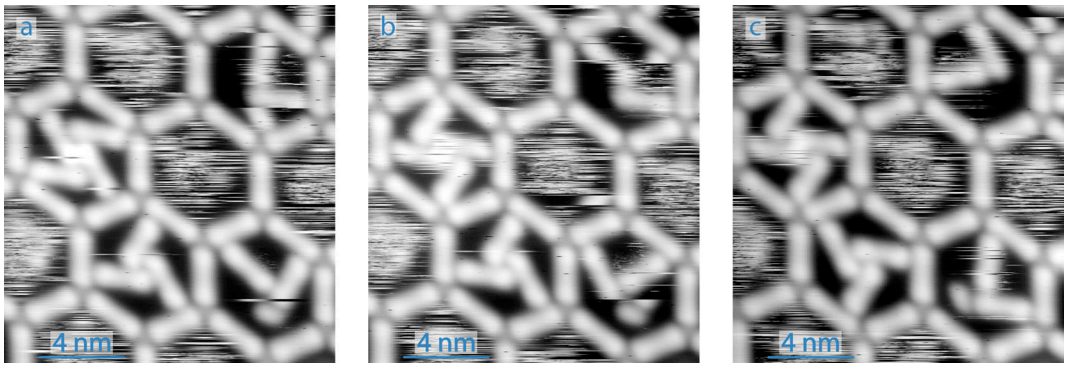

Fig. S4: (a-c) Simultaneous observation of the movement of a confined monomer, dimer, trimer and tetramer. In the temperature region where the motions of the trimer and tetramer set in, the three topographs have been recorded subsequently with a time lap of 283 and 291 s, respectively. The tetramer performs a motion of 60° counterclockwise (a→b). Subsequently, the trimer performs a rotational motion (b→c). On the top right there are two molecules within the cavity joined by a hydrogen bond to a dimer. The angle the two molecules enclose varies. Therefore, the motions of the dimeric molecular unit represent combined rotational and translational molecular movements, which in general similarly applies to the tetramer. Close to the center of the images there is a cavity merely occupied by a single molecule performing numerous changes of its adsorption site. Because the monomer becomes doubly bound to the cavity rim in (b), the motion of the monomer is interrupted for 6.6 s at the lower right corner of the hexagon. The more bonds a molecular guest unit maintains, the more dilatory its motion is (V_B = 2 V, I_T = 0.1 nA, T_{Sample} = 60.7 – 60.9 K).